Ordered Arrays of Vertically Aligned [110] Silicon Nanowires by Suppressing the Crystallographically Preferred Etching Directions

ARTICLE *in* NANO LETTERS · JUNE 2009

Impact Factor: 13.59 · DOI: 10.1021/nl803558n · Source: PubMed

8 AUTHORS, INCLUDING:

Zhipeng Huang
Jiangsu University
49 PUBLICATIONS **1,770** CITATIONS
SEE PROFILE

Tomohiro Shimizu
Kansai University
82 PUBLICATIONS **779** CITATIONS
SEE PROFILE

Zhang Zhang
South China Normal University
21 PUBLICATIONS **242** CITATIONS
SEE PROFILE

Nadine Geyer
Carl Zeiss Jena GmbH
21 PUBLICATIONS **833** CITATIONS
SEE PROFILE

NANO LETTERS

2009
Vol. 9, No. 7
2519-2525

Ordered Arrays of Vertically Aligned [110] Silicon Nanowires by Suppressing the Crystallographically Preferred <100> Etching Directions

Zhipeng Huang,*,† Tomohiro Shimizu,† Stephan Senz,† Zhang Zhang,† Xuanxiong Zhang,†,‡ Woo Lee,†,§ Nadine Geyer,† and Ulrich Gösele*,†

Max Planck Institute of Microstructure Physics, Weinberg 2, D-06120 Halle, Germany, Korea Research Institute of Standards and Science (KRISS), Yuseong, 305-340 Daejon, Korea, and Institute of Microelectronics, Chinese Academy of Sciences, 100029, Beijing, China

Received November 24, 2008; Revised Manuscript Received January 15, 2009

ABSTRACT

The metal-assisted etching direction of Si(110) substrates was found to be dependent upon the morphology of the deposited metal catalyst. The etching direction of a Si(110) substrate was found to be one of the two crystallographically preferred ⟨100⟩ directions in the case of isolated metal particles or a small area metal mesh with nanoholes. In contrast, the etching proceeded in the vertical [$\bar{1}\bar{1}$0] direction, when the lateral size of the catalytic metal mesh was sufficiently large. Therefore, the direction of etching and the resulting nanostructures obtained by metal-assisted etching can be easily controlled by an appropriate choice of the morphology of the deposited metal catalyst. On the basis of this finding, a generic method was developed for the fabrication of wafer-scale vertically aligned arrays of epitaxial [110] Si nanowires on a Si(110) substrate. The method utilized a thin metal film with an extended array of pores as an etching catalyst based on an ultrathin porous anodic alumina mask, while a prepatterning of the substrate prior to the metal depostion is not necessary. The diameter of Si nanowires can be easily controlled by a combination of the pore diameter of the porous alumina film and varying the thickness of the deposited metal film.

One-dimensional (1D) materials are intriguing building blocks for applications in the fields of electronics and photonics. Special focus has been put on silicon nanowires (SiNWs) due to their promising application potential ranging from advanced electronic devices,[1,2] optoelectronic devices,[3,4] to biological and chemical sensors,[5,6] and to renewable energy devices.[7] As with many 1D materials, the properties of the SiNWs vary with parameters such as crystallographic orientation,[8,9] diameter,[10] surface,[11,12] and strain.[8,13] Besides the intrinsic properties, the direction of the SiNWs relative to the substrate surface is an important factor for SiNWs-based devices, such as inclined-SiNW-based solar cells[14] and vertical-SiNW-based field effect transistors (FETs).[1,2] Great efforts have been devoted to fabricating SiNWs with controllable crystallographic orientation, diameter, position, and direction relative to the substrate surface.

SiNWs with [110] orientation are of special importance for future electronic devices since a significant enhancement of hole and electron mobilities was observed in [110] SiNWs compared to [100] SiNWs with comparable diameters.[9] A high carrier mobility is crucial for high-speed FETs.[15] Surround-gate FETs based on vertically aligned SiNWs are particularly promising because short-channel effects can be reduced compared to double gate devices and better electrostatic gate control of the conducting channel and a significant increase of the transistor density per unit area can be achieved.[1,2] Therefore, vertically aligned [110] SiNWs have the potential to play an important role in future high-speed and high-density FET devices.

However, fabrication of vertically aligned [110] SiNWs is difficult to achieve by the conventional vapor−liquid−solid (VLS) method despite the preferential growth along ⟨110⟩ directions especially for SiNWs with small diameters.[16,17] According to the configuration of the ⟨110⟩ family of directions, even if Si(110) is used as a substrate and the diameter of the SiNWs is well controlled, inclined ⟨110⟩ SiNWs, for example, [011] SiNWs, for which their wire axis deviates 60° from the substrate normal, were inevitably grown beside the vertically aligned [110] SiNWs. In addition,

* To whom correspondence should be addressed: Zhipeng Huang, zhuang@mpi-halle.mpg.de; Ulrich Gösele, goesele@mpi-halle.mpg.de.
† Max Planck Institute of Microstructure Physics.
‡ Institute of Microelectronics, Chinese Academy of Sciences.
§ Korea Research Institute of Standards and Science.

10.1021/nl803558n CCC: $40.75
Published on Web 05/29/2009

SiNWs obtained from the VLS method contain metallic impurities from the catalyst used such as gold, which are detrimental to the performance of nanodevices.[18]

As a low-cost alternative method, metal-assisted chemical etching of Si could be a promising solution for fabricating SiNWs and other Si nanostructures.[19−24] In metal-assisted chemical etching, isolated nanoparticles or meshlike porous films of noble metals (e.g., silver, gold, or platinum) deposited on a Si substrate are used as catalyst to assist etching of Si in an etching solution containing HF and an oxidant (e.g., H_2O_2). The Si below the areas covered with the metal is etched much faster than the bare surface, yielding porous Si or arrays of SiNWs depending on the geometry of the deposited metal catalyst.[20,25] Nanoporous Si with oriented pores can be obtained, when isolated metal nanoparticles are used as a catalyst. On the other hand arrays of SiNWs can be produced, when a thin metal mesh with a patterned array of nanoholes is used as a catalyst. In general, the directions along which the etching proceeds are strongly dependent on the crystallographic orientation of the Si substrate. Si substrates with (100),[20,23] (110),[26−28] or (111)[14,25] orientation exhibit a preferred etching along ⟨100⟩ directions. Various cases of etching of Si(110) substrates with a catalytic metal mesh were reported to result in ⟨100⟩ SiNWs inclined to the substrate surface.[26−28]

Therefore, it is desirable to develop a method for fabricating vertically aligned [110] SiNWs. In this Letter, we report on a systematic study on the etching behavior of the Si(110) substrate and a novel method for the fabrication of vertically aligned [110] SiNW arrays. We found that the etching direction of the Si(110) substrate depends on the morphology of the deposited metal catalyst, which has not been reported so far. In the case of isolated metal nanoparticles, the etching of Si(110) occurs along ⟨100⟩ directions irrespective of the size of the metal particles. On the other hand, the etching direction was found to depend on the lateral dimension of the catalytic metal film in the case of a metal mesh with predefined arrays of holes: the etching proceeds along ⟨100⟩ directions for small area silver meshes, while $[\bar{1}\bar{1}0]$ is the preferred etching direction for large area ones. An ultrathin anodic aluminum oxide (AAO) membrane was utilized as a mask for the patterning of the metal film with ordered arrays of holes. The resulting metal mesh on the AAO membrane was used as a catalyst in wet etching of a Si(110) substrate to fabricate vertically aligned extended arrays of epitaxial [110] SiNWs on a wafer scale. In this method, the spacing (i.e., density) between SiNWs is predefined by the interpore distance of the porous AAO membrane which can be conveniently varied in the range of 60−500 nm by choosing appropriate anodization conditions. The diameter of SiNWs is readily controlled by a combination of the pore diameter in the alumina mask and a variation of the thickness of the metal mesh. In addition, prepatterning of a Si substrate by reactive ion etching (RIE) process is not necessary, which had to be employed to obtain the catalytic metal mesh by sputtering of the metal layer in our previously reported method.[24] Moreover, the present method should not be limited to Si(110) substrates and should be easily extended to Si substrates with other orientations and possibly even polycrystalline silicon solar cell material, enabling economic and controlled fabrication of vertically aligned SiNWs with desired diameter and crystallograpic orientations.

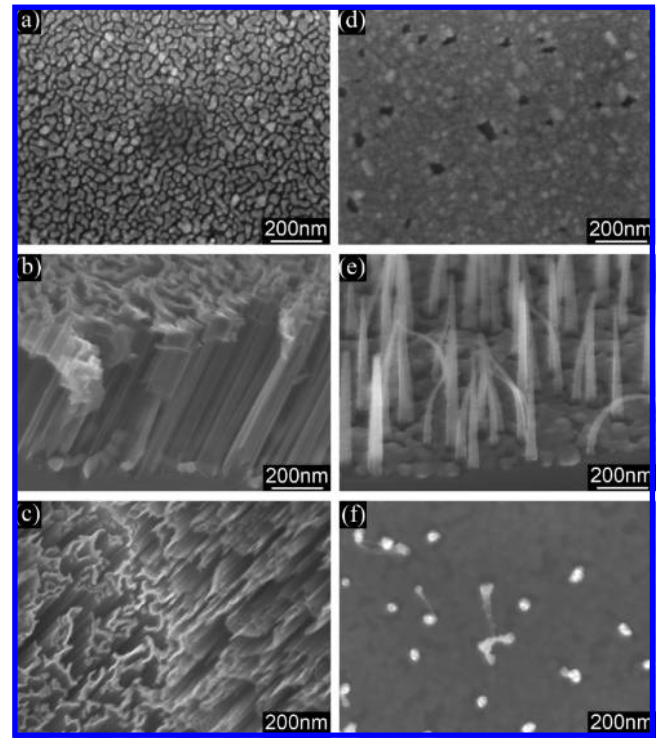

Figure 1. (a) SEM image of 5 nm thick (nominal thickness) silver deposited by sputtering on the (110) substrate. (b) Bird's-eye view and (c) plan-view SEM images of the substrate etched with 5 nm thick silver. (d) SEM image of 10 nm thick (nominal thickness) silver deposited by sputtering on the (110) substrate. (e) Bird's-eye view and (f) plan-view SEM images of the substrate etched with 10 nm thick silver.

Figure 1 illustrates the effect of metal film morphology on the evolution of Si nanostructures upon metal-assisted chemical etching of n-type Si(110) substrates. Thin layers of catalytic silver with different nominal thicknesses were deposited directly on Si(110) substrates by sputtering deposition prior to etching. The morphology of the silver film was found to depend on its thickness and varied from isolated nanoparticles, isolated patches, interconneted patches, a continuous film with nanopores, to a continuous film without pores. The morphology of a 5 nm thick silver film is characterized by isolated patches with irregular shapes (Figure 1a), while a continuous layer of metal with randomly distributed pores is present in the case of a 10 nm thick silver film (Figure 1d). Metal-assisted chemical etching was carried out by immersing the silver-coated Si(110) substrates into a mixture solution of HF, H_2O_2, and H_2O (v/v/v = 10/2.5/37.5) for 5 min (see Supporting Iinformation for more details). The morphologies of the resulting samples were investigated by scanning electron microscopy (SEM). It is apparent from panels b, c, e, and f of Figure 1 that the direction of etching is dependent on the morphology of the deposited silver. In the case of isolated patches of silver, the Si(110) substrate was etched in oblique directions and resulted in inclined SiNWs or nanowalls (Figure 1b,c). On

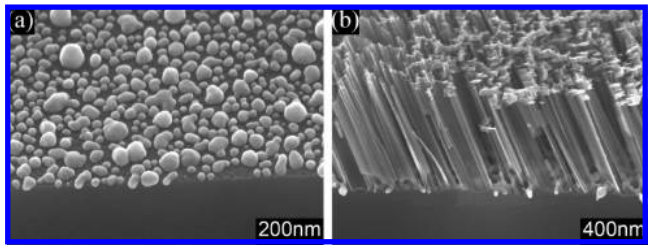

Figure 2. (a) Bird's-eye view SEM image of the electroless deposited silver particles on a (110) substrate. (b) Bird's-eye view SEM images of the substrate etched with electroless deposited silver particles.

the other hand, the substrate was etched in the vertical direction yielding SiNWs whose wire axes are perpendicular to the surface of the substrate (Figure 1e,f). Vertically aligned SiNWs exhibit a tapered shape (Figure 1e), which could be attributed to lateral etching of individual SiNWs by the etching solution[29,30] and/or to a gradual widening of the metal nanoholes due to partial dissolution of silver by the etching solution. Some of the SiNWs appear to be bent and stuck to each other, which is due to the surface tension force exerted on the nanowires during the drying of the sample (i.e., an evaporation process of the solvent).[31]

As a comparative experiment, isolated silver nanoparticles were used as catalysts in metal-assisted chemical etching of a Si(110) substrate. Silver nanoparticles were directly deposited on the substrate by an electroless displacement reaction in a solution comprising Ag^+ and HF for 30 s (Figure 2a). Subsequently, the resulting Ag-loaded Si(110) substrate was etched under the same condition as that employed for the samples shown in Figure 1. As manifested by Figure 2b, etching took place in a inclined manner to the substrate surface similar to the case of eching by isolated patches of silver films with irregular shapes shown in Figure 1b, which clearly indicates that the orientation of the Si substrate influences the direction of etching (with respect to the surface orientation) for the case of isolated silver. The direction of etching was not altered, even if we employed silver catalysts that were deposited by increasing the time of displacement reaction to 150 s in order to increase the size of the silver deposits. This experimental observation is in line with the recent results by Yen et al. who showed anisotropic etching along the ⟨100⟩ directions (i.e., inclined etching) for etching of a Si(110) substrate in Ag^+/HF solution for 40 min.[27] In addition, it implies that electroless silver deposits prefer to form three-dimensional (3D) dendritic structures rather than two-dimensional (2D) continuous films with pores.[32,33] Accordingly, one cannot obtain vertically aligned SiNWs on a Si(110) substrate, if silver formed by electroless deposition is used as a catalyst in metal-assisted chemical etching.

Representative cross-sectional transmission electron microscopy (TEM) images of Si(110) substrates that were etched by using isolated silver nanoparticles and a silver mesh with nanoholes are shown in panels a and b of Figure 3, respectively. Selected area electron diffraction (SAED) patterns of the respective samples are shown as insets. Figure 3c depicts schematically the definition of the crystallographic directions of the Si(110) substrate. It is apparent from the TEM images and the corresponding SAED patterns that there are two distinct etching behaviors depending on the morphological details of the deposited catalytic silver.[34] In the case of isolated silver particles, metal-assisted chemical etching of Si(110) substrate takes place along the $[0\bar{1}0]$ direction to generate inclined nanowire arrays (Figure 3a), which is a preferred crystallographic direction according to the back-bond theory.[26−28] On the other hand, etching of a Si(110) substrate by a catalytic silver mesh takes place along the $[\bar{1}\bar{1}0]$ direction and generates arrays of SiNWs perpendicular to the substrate surface (Figure 3b). The present experimental findings demonstrate that the etching behavior cannot fully be explained by just simple crystallographic considerations. The observed vertical etching of Si(110) substrates by a catalytic silver mesh can be understood by considering the etching kinetics under geometric constraints, as will be discussed below.

Upon close examination of TEM images shown in Figure 3, we found that the vertical displacements of catalytic silver along the $[\bar{1}\bar{1}0]$ direction are almost the same for the same period of etching time (i.e., 5 min) irrespective of morphological details of the deposited catalytic silver (i.e., 525 nm for isolated silver particles and 510 nm for the silver mesh with arrays of nanoholes). Moreover, similar to what happens in vertical etching, the lateral direction of the isolated silver patches remains parallel to the substrate surface during the inclined etching (Figure S1 in Supporting Information). These aspects of the etching behavior along the $[\bar{1}\bar{1}0]$ direction for the inclined etching are identical to that for the vertical etching. Formally, the inclined ⟨100⟩ etching can be regarded as a vectorial addition of lateral (i.e., $[1\bar{1}0]$ or $[\bar{1}10]$) and vertical (i.e., $[\bar{1}\bar{1}0]$) etching. Therefore, the vertical etching of Si(110) assisted by the silver mesh results from the restriction of lateral etching, which is a morphological effect of the interconnected silver mesh.

At the initial stage of etching, isolated silver particles can move freely and etch the substrate along one of the two crystallographically preferred $[\bar{1}00]$ or $[0\bar{1}0]$ directions at random (Figure 4a). In contrast, with increasing etching time the particles switch their etching directions and move in the same direction as their neighbors (Figure 1b, Figure 2b). Therefore, a well-defined domain structure develops in which the etching has the same direction within a given domain (Figure 1c). Moreover, the silver particles near the domain boundary switch their directions in sequence, leading to the coalescence of domains and the enlargement of the size of domains in which the SiNWs show an unidirectional alignment (Figure 4b). This phenomenon implies that there is a distance-dependent interaction between the silver particles which makes the silver particles cooperatively move in the same direction. The origin of such interaction is not understood at the moment. Possible reasons might be image forces between the silver particles,[35] or/and the influence of band bending at the silver/Si interface from neighboring silver particles which influences carrier transfer through the silver/Si interface.[36] Influenced by such interactions, the size

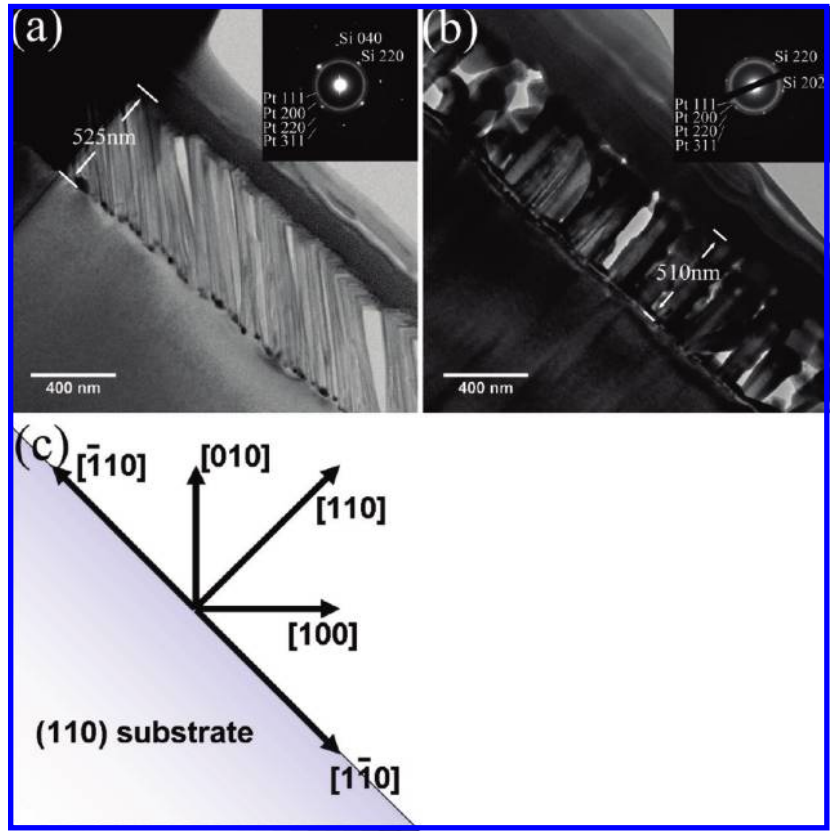

Figure 3. The cross-sectional TEM images of (a) the slantingly etched substrate and (b) the vertically etched substrate. The insets show the SAED patterns from the etched structures. Diffraction rings in the insets of panels a and b come from platinum particles that were deposited to protect the samples during focused-ion-beam milling. (c) Definition of directions used in the text.

of domains can be larger than 100 μm in a sample etched for 10 min (Figure S2 in Supporting Information).

For a silver mesh, different parts of the mesh tend to move along the [$\bar{1}$00] or [0$\bar{1}$0] directions at random, depending on the defect sites on the surface of the substrate,[37] the shape or profile at the edge of the silver pores or the silver mesh,[38,39] and the interaction between the substrate and the silver particles.[28] Meanwhile, the interaction between silver particles tends to make the silver particles move in the same direction. If the interaction extends over the entire mesh, the entire mesh does move in the same inclined direction during etching provided the lateral size of the interconnected mesh is small (Figure S3 in Supporting Information). In contrast, if the lateral size of the mesh is sufficiently large so that the interaction could not extend over the whole mesh, the different parts of the mesh will maintain the tendencies to move along allowable etching directions in random. However, the interconnected silver particles in an interconnected silver film cannot move freely like the isolated particles. As a compromise among conflicting lateral etching directions ([1$\bar{1}$0] and [$\bar{1}$10]), the lateral motion of the large-area silver mesh is elimated, and the large-area silver mesh can only move in a common vertical direction ([$\bar{1}\bar{1}$0]), leading to vertically aligned [110] SiNWs. Our suggested mechanism for the vertical etching is confirmed by the fact that the vertical etching can be converted to the inclined etching due to a splitting of a large-area silver film into many smaller pieces induced by the dissolution of the silver during the etching (Figure S4 in Supporting Information).

The results show that the crystallographically preferred etching can be suppressed simply by introducing a morphological constraint. The morphology-dependent etching works on both n-type and p-type Si(110) substrates. On the basis of these results, we developed a simple method to fabricate highly ordered vertically aligned [110] SiNW arrays on Si(110) substrates. Figure 5 shows a schematic of the fabrication processes. An ultrathin porous AAO membrane was used as a patterning mask to deposit a large-area metal film with ordered arrays of pores, and further to define position, shape, and diameter of the SiNWs. First, an AAO/polystyrene (PS) membrane, as large as 1 $\times$ 1 cm^2, was transferred onto the Si(110) substrate (Figure 5a).[40] Subsequently, the PS that was used to stabilize the AAO membrane during transfer of the AAO membrane onto the Si substrate was removed by oxygen plasma, chloroform rinsing, or a simple heat treatment (Figure 5b). Then, a thin layer of silver film was deposited onto the AAO membrane by sputtering. With the AAO membrane as a scaffold, the silver formed a continuous film with orderly distributed pores (Figure 5c). After the deposition, the silver-coated AAO/Si was immersed into an etching solution composed of HF, H_2O_2, and H_2O. This process resulted in complete dissolution of the ultrathin AAO membrane, and thus the silver film came in contact with the underlying Si substrate. The large-area silver film etched the Si substrate to produce extended arrays of

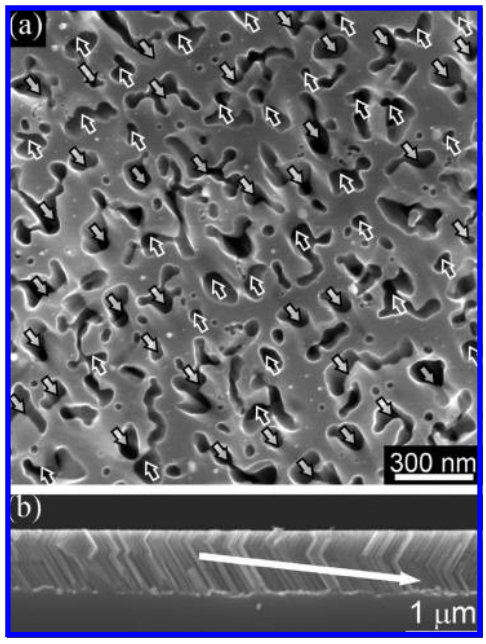

Figure 4. (a) Plan-view SEM image showing the morphology of (110) substrate etched by large-distance isolated silver particles, in which the arrows indicate the initial etching direction (etching time 2 min). (b) Cross-sectional SEM image showing that the silver particles switch their moving directions from left to right in sequence. The arrow shows the propagation direction (etching time 5 min).

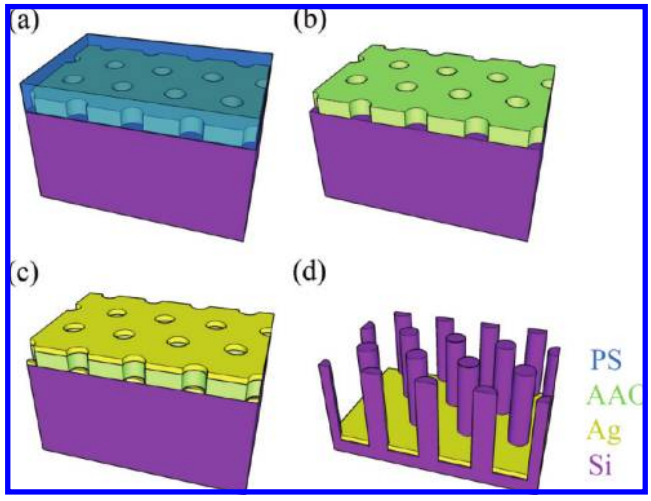

Figure 5. Schematic of the fabrication process for vertically aligned [110] SiNWs arrays. (a) AAO/PS mask on a (110) Si substrate through an AAO transfer process,[40] in which the PS is deposited prior to the transfer in order to protect the AAO membrane during the removal of the barrier layer and offer a hydrophobic surface during the AAO transfer process. (b) Removal of PS by O_2 plasma treatment. (c) Deposition of a silver mesh by sputtering. After the deposition, the silver-coated AAO/Si is immersed into an etching solution. This process results in complete dissolution of the ultrathin AAO membrane, and thus the silver mesh comes in contact with the underlying Si substrate. (d) Catalyzed by the silver mesh, the Si substrate is chemically etched to form vertically aligned [110] SiNWs.

vertically aligned [110] SiNWs (Figure 5d). After the etching, the silver film could be removed by dipping the sample into HNO_3 solution.

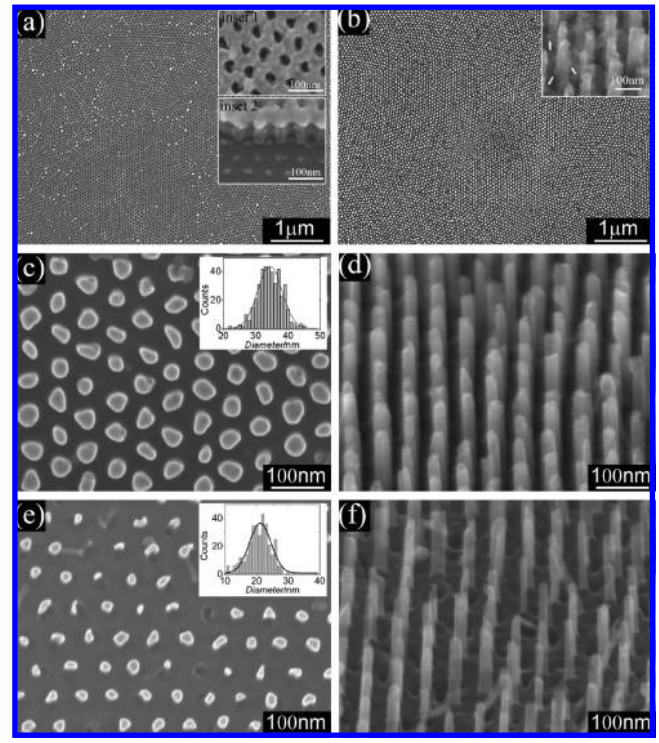

Figure 6. (a) Plan-view SEM image of the silver-coated AAO membrane on the (110) Si substrate. Inset 1 shows a plan-view high-resolution SEM image of the same sample, and insert 2 shows a bird's-eye view SEM image of the sample on which the AAO was partly removed. (b) Plan-view SEM image of the vertical [110] SiNW arrays after silver removal, the inset shows a bird's-eye view SEM image of the vertical [110] SiNWs before silver removal. (c) Plan-view and (d) bird's-eye view SEM images of the vertical [110] SiNW arrays etched with a 15 nm thick silver film for 120 s. The inset of (c) shows the diameter distribution of SiNWs fabricated with a 15 nm thick silver film. (e) Plan-view and (f) bird's-eye view SEM images of the vertical [110] SiNW arrays etched with a 20 nm thick silver film for 90 s. The inset of (e) shows the diameter distribution of SiNWs fabricated with a 20 nm thick silver film. The bars in the inset of (c, e) represent the measured statistical data and the solid lines are Gaussian fits.

Figure 6a shows an SEM image of the silver-coated AAO membrane on a p-type Si(110) substrate. The insets show high-resolution plan-view and bird's-eye view SEM images of the membrane, respectively. Figure 6b presents a plan-view SEM image of the large-area highly ordered [110] SiNW arrays after removal of silver by HNO_3 treatment. The inset shows a bird's-eye view SEM image of [110] SiNW arrays before removal of silver. After the silver deposition, silver was also deposited on the Si substrate at the bottom of the pores in the AAO membrane and not only at the top surface of the AAO membrane (inset 2, Figure 6a). The etching rate of the silver particles is slower than that of the silver film.[24] Therefore, after etching the Si initially below the isolated silver particles are transformed into SiNWs. Moreover, due to the closure effect the diameter of the silver particles loading on the Si substrate is smaller than the diameter of apertures in the AAO membrane.[41] Accordingly, during the etching process the silver particles might detach from the Si substrate and go into the solution through the apertures, leaving behind the Si initially below the silver particles as SiNWs. Consequently, silver particles can rarely

be found on the top of the SiNWs (inset of Figure 6b). The small silver particles on the sidewall of the SiNWs, indicated by arrows in the inset of Figure 6b, might come from the particles detached from the silver film, which is similar to the SiNWs shown in Figure 1e.

Panels c and d of Figure 6 show the plan-view and bird's-eye view SEM images of the SiNW arrays fabricated with a 15 nm thick silver film. The silver was removed. As shown by the inset 1 of Figure 6a, the apertures on the silver film are not all circular due to the irregular shape of pores in the AAO membrane. In general, the cross-sectional shape of the SiNWs was determined by the shape of apertures on the silver film; therefore the irregular shapes of apertures in the silver film lead to the irregular cross-sectional shapes of the SiNWs (Figure 6c). Circular SiNWs can be obtained if pore-widening of the AAO membrane is carried out before the silver deposition. Due to the closure effect, the diameter of apertures in the silver film will decrease if the thickness of the silver film is increased.[41] The diameter of the SiNWs in metal-assisted chemical etching is known to be determined by the size of pores in the metal film. Therefore, the diameter of the [110] SiNWs can simply be decreased by increasing the thickness of the silver film. Panels e and f of Figure 6 show the plan-view and bird's-eye view SEM images of the SiNW arrays fabricated with a 20 nm thick silver film. The insets of panels c and e of Figure 6 show the diameter distributions of SiNWs etched with the 15 and 20 nm thick silver films, respectively, in which the diameters were measured from the plan-view SEM images. It is shown by Gaussian fitting of the diameter distributions that the average diameter of SiNWs decreases from 34 ± 4 to 21 ± 3 nm with increasing the thickness of the silver film from 15 to 20 nm.

In summary, we have studied the metal-assisted chemical etching behavior of Si(110) substrates and found that the two crystallographically preferred ⟨100⟩ etching directions can be suppressed by the presence of a sufficiently laterally extended metal film. By variation of the morphology of the deposited metal used to assist the etching, inclined or vertical etching can be achieved. On the basis of the morphology-dependent etching, we developed a novel and simple method to fabricate vertically aligned [110] SiNW arrays. The method used directly the AAO membrane as the mask for depositing the silver film. Large-area highly ordered epitaxial [110] SiNW arrays were fabricated by this approach. The diameter of SiNWs could be simply controlled by a combination of the pore diameter of the alumina template combined and a variation of the thickness of the silver film used to assist the etching.

Acknowledgment. Financial support from the German Research Foundation (STE 1127/8-1) is greatly acknowledged. We also acknowledge support by the European project NODE (IST 015783) and the German-Israel DIP-projects K6.1 managed by the German Research Foundation (DFG) under Contract Number GO 704_5-1. This work was partly supported by New & Renewable Energy R&D program under the Korea Ministry of Commerce, Industry and Energy (MOCIE).

Supporting Information Available: Experimental details and TEM sample preparation, relationship between lateral direction of silver patches and the surface of the Si substrate in the inclined etching case, large-area domain in which the inclined SiNWs have the same aligned direction, lateral etching and the influence of the lateral size of the silver film, and switch of etching direction during etching. This material is available free of charge via the Internet at http://pubs.acs.org.

References

(1) Schmidt, V.; Riel, H.; Senz, S.; Karg, S.; Riess, W.; Gösele, U. *Small* **2006**, *2*, 85–88.
(2) Goldberger, J.; Hochbaum, A. I.; Fan, R.; Yang, P. *Nano Lett.* **2006**, *6*, 973–977.
(3) Peng, K. Q.; Xu, Y.; Wu, Y.; Yan, Y. J.; Lee, S. T.; Zhu, J. *Small* **2005**, *1*, 1062–1067.
(4) Tian, B.; Zheng, X.; Kempa, T. J.; Fang, Y.; Yu, N.; Yu, G.; Huang, J.; Lieber, C. M. *Nature* **2007**, *449*, 885–890.
(5) Cui, Y.; Wei, Q.; Park, H.; Lieber, C. M. *Science* **2001**, *293*, 1289–1292.
(6) Patolsky, F.; Zheng, G.; Lieber, C. M. *Nat. Protoc.* **2006**, *1*, 1711–1724.
(7) Chan, C. K.; Peng, H.; Liu, G.; McIlwrath, K.; Zhang, X. F.; Huggins, R. A.; Cui, Y. *Nat. Nanotechnol.* **2008**, *3*, 31–35.
(8) Hong, K. H.; Kim, J.; Lee, S. H.; Shin, J. K. *Nano Lett.* **2008**, *8*, 1335–1340.
(9) Buin, A. K.; Verma, A.; Svizhenko, A.; Anantram, M. P. *Nano Lett.* **2008**, *8*, 760–765.
(10) Ma, D. D. D.; Lee, C. S.; Au, F. C. K.; Tong, S. Y.; Lee, S. T. *Science* **2003**, *299*, 1874–1877.
(11) Leao, C. R.; Fazzio, A.; da Silva, A. J. R. *Nano Lett.* **2007**, *7*, 1172–1177.
(12) Hochbaum, A. I.; Chen, R. K.; Delgado, R. D.; Liang, W. J.; Garnett, E. C.; Najarian, M.; Majumdar, A.; Yang, P. D. *Nature* **2008**, *451*, 163–U5.
(13) Lyons, D. M.; Ryan, K. M.; Morris, M. A.; Holmes, J. D. *Nano Lett.* **2002**, *2*, 811–816.
(14) Fang, H.; Li, X. D.; Song, S.; Xu, Y.; Zhu, J. *Nanotechnology* **2008**, *19*, 255703.
(15) Haensch, W.; Nowak, E. J.; Dennard, R. H.; Solomon, P. M.; Bryant, A.; Dokumaci, O. H.; Kumar, A.; Wang, X.; Johnson, J. B.; Fischetti, M. V. *IBM J. Res. Dev.* **2006**, *50*, 339–361.
(16) Wu, Y.; Cui, Y.; Huynh, L.; Barrelet, C. J.; Bell, D. C.; Lieber, C. M. *Nano Lett.* **2004**, *4*, 433–436.
(17) Schmidt, V.; Senz, S.; Gösele, U. *Nano Lett.* **2005**, *5*, 931–935.
(18) Bailly, A. R., O.; Barrett, N.; Zagonel, L. F.; Gentile, P.; Pauc, N.; Dhalluin, F.; Baron, T.; Chabli, A.; Cezar, J. C.; Brookes, N. B. *Nano Lett.* **2008**, *8*, 3709–3714.
(19) Li, X.; Bohn, P. W. *Appl. Phys. Lett.* **2000**, *77*, 2572–2574.
(20) Peng, K. Q.; Yan, Y. J.; Gao, S. P.; Zhu, J. *Adv. Mater.* **2002**, *14*, 1164–1167.
(21) Tsujino, K.; Matsumura, M. *Adv. Mater.* **2005**, *17*, 1045−+.
(22) Huang, Z. P.; Wu, Y.; Fang, H.; Deng, N.; Ren, T. L.; Zhu, J. *Nanotechnology* **2006**, *17*, 1476–1480.
(23) Huang, Z. P.; Fang, H.; Zhu, J. *Adv. Mater.* **2007**, *19*, 744–748.
(24) Huang, Z. P.; Zhang, X. X.; Reiche, M.; Liu, L. F.; Lee, W.; Shimizu, T.; Senz, S.; Gösele, U. *Nano Lett.* **2008**, *8*, 3046–3051.
(25) Peng, K. Q.; Wu, Y.; Fang, H.; Zhong, X. Y.; Xu, Y.; Zhu, J. *Angew. Chem., Int. Ed.* **2005**, *44*, 2737–2742.
(26) Peng, K. Q.; Zhang, M. L.; Lu, A. J.; Wong, N. B.; Zhang, R. Q.; Lee, S. T. *Appl. Phys. Lett.* **2007**, *90*, 163123.
(27) Chen, C. Y.; Wu, C. S.; Chou, C. J.; Yen, T. J. *Adv. Mater.* **2008**, *20*, 3811–3815.
(28) Peng, K. Q.; Lu, A. J.; Zhang, R. Q.; Lee, S. T. *Adv. Funct. Mater.* **2008**, *18*, 3026–3035.
(29) Lee, C. L.; Tsujino, K.; Kanda, Y.; Ikeda, S.; Matsumura, M. *J. Mater. Chem.* **2008**, *18*, 1015–1020.
(30) Zhang, M. L.; Peng, K. Q.; Fan, X.; Jie, J. S.; Zhang, R. Q.; Lee, S. T.; Wong, N. B. *J. Phys. Chem. C* **2008**, *112*, 4444–4450.
(31) Zhu, K.; Vinzant, T. B.; Neale, N. R.; Frank, A. J. *Nano Lett.* **2007**, *7*, 3739–3746.
(32) Peng, K. Q.; Yan, Y. J.; Gao, S. P.; Zhu, J. *Adv. Funct. Mater.* **2003**, *13*, 127–132.
(33) Peng, K. Q.; Zhu, J. *Electrochim. Acta* **2004**, *49*, 2563–2568.

(34) Comparing the thicknesses of catalytic silver in Figure 1 and Figure 2, we can rule out a possible thickness effect of catalytic silver on the different etching behaviors.
(35) You, S.; Choi, M. *J. Aerosol Sci.* **2007**, *38*, 1140–1149.
(36) Sullivan, J. P.; Tung, R. T.; Pinto, M. R.; Graham, W. R. *J. Appl. Phys.* **1991**, *70*, 7403–7424.
(37) Zhang, X. G., *Electrochemistry of Silicon and Its Oxide*; Kluwer Academic/Plenum Publisher: New York, 2001.
(38) Tsujino, K.; Matsumura, M. *Electrochem. Solid State Lett.* **2005**, *8*, C193−C195.
(39) Tsujino, K.; Matsumura, M. *Electrochim. Acta* **2007**, *53*, 28–34.
(40) Lee, W.; Han, H.; Lotnyk, A.; Schubert, M. A.; Senz, S.; Alexe, M.; Hesse, D.; Baik, S.; Gösele, U. *Nat. Nanotechnol.* **2008**, *3*, 402–407.
(41) Lei, Y.; Chim, W. K. *Chem. Mater.* **2005**, *17*, 580–585.

NL803558N